

Article

Active Control Method Based on Equivalent Stiffness and Damping Coefficient for an Electromagnetic Isolation System

Lei Zhang ^{1,2} and Xiangtao Zhuan ^{3,4,*} 

¹ The Key Laboratory of Metallurgical Equipment and Control of Education Ministry, Wuhan University of Science and Technology, Wuhan 430081, China; leizh@wust.edu.cn

² Hubei Key Laboratory of Mechanical Transmission and Manufacturing Engineering, Wuhan University of Science and Technology, Wuhan 430081, China

³ Department of Artificial Intelligence and Automation, School of Electrical Engineering and Automation, Wuhan University, Wuhan 430072, China

⁴ Shenzhen Research Institute, Wuhan University, Shenzhen 518057, China

* Correspondence: xtzhuan@whu.edu.cn; Tel.: +86-027-6877-2477

Received: 20 October 2020; Accepted: 5 November 2020; Published: 10 November 2020



Abstract: For improving the performance of an electromagnetic isolation system with reasonable parameters and avoid the parameter tuning problem of a PID controller, an active control method is put forward based on equivalent stiffness and damping coefficient. In this paper, the range of equivalent stiffness coefficient and damping coefficient of the electromagnetic force are calculated based on the required range of dynamic performance indexes. According to the nonlinear expression between electromagnetic force and coil current and gap, the relationships between the coil current and equivalent stiffness coefficient and damping coefficient are established. Then, the equivalent stiffness coefficient and damping coefficient can be satisfied by the controlled current in different gaps for meeting the required dynamic performance indexes. For reducing the maximum overshoot and the number of oscillations of the system, the active control method with the piecewise equivalent stiffness and damping coefficient is proposed based on the piecewise control strategy to realize the variable control parameters of the isolation system. Simulation and experimental results verify that the control method based on the equivalent stiffness and damping coefficient can obtain the desired dynamic performance indexes and the proposed control method with the piecewise strategy can not only reduce the setting time of the system, but also ensure the stability of the system.

Keywords: active control; vibration isolation; equivalent stiffness; equivalent damping

1. Introduction

Vibration, a ubiquitous physical phenomenon in the field of engineering and technology, has brought many inconveniences and hazards to daily life, scientific research, and production. For example, vibrations may reduce the processing accuracy and the surface finish of the workpieces, affect the accuracy of precision equipments, cause the chatter of aircrafts and ship hulls, and decrease the life of mechanical systems [1,2]. In recent years, high requirement on vibration control has been paid in processing equipments, measuring instruments, mechanical systems, and other engineering applications. Therefore, an effective vibration isolation system should be developed [3,4].

In recent years, a lot of vibration isolation systems have been developed and exploited effectively to control vibration. Vibration isolation systems can be divided into two kinds in general: passive isolation systems and active isolation systems [5,6]. Passive isolation systems cannot require external power sources and control systems during the action, which operate with negative work to consume the kinetic energy for vibration isolation systems [7–9]. They have been extensively used to isolate vibration because of the simple structure and the low cost [10–12].

The aforementioned passive isolation systems can effectively isolate vibration without any external power and control systems. However, the fixed-structure parameters (stiffness and damping coefficient) of passive isolation systems fail to meet the high requirements on various dynamic performances. In comparison with passive isolation systems, active electromagnetic isolation systems can effectively solve these problems with controllable stiffness and damping coefficient to achieve dynamic performance indexes based on various control methods. Lots of active electromagnetic isolation systems have been designed and utilized to control vibration. Kim et al. designed the vibration isolation system to provide the electro-magnetic levitation force based on the magnetic actuator and the pneumatic elastic chamber for semiconductor processing equipments [13]. Zhou et al. developed a novel vibration isolation system with a mechanical spring, two electromagnets, and a permanent magnet which are built for a magnetic spring [14]. In order to overcome the problems of the passive isolation systems, Ahn et al. presented a hybrid-type isolation system based on the electromagnetic and pneumatic force for mechanical systems [15].

Although many methods have been developed and used effectively for designing active isolation systems, active control methods should be studied due to the fact that the controller can improve the performance of vibration isolation systems. According to different application conditions and requirements on vibration control accuracy, different control strategies and algorithms are needed to design the controller of an active vibration isolation system. At present, the control methods of active vibration isolation systems mainly include direct output feedback, adaptive control, optimal control, neural network control, and so on. Sun et al. proposed a fuzzy controller for a vibration isolation system disturbed by regular excitation signals [16]. Bai et al. employed linear quadratic gaussian control and μ -synthesis in the controller for the active isolation system [17]. Shaw et al. employed an adaptive controller for actively controlling an actuator for vibration isolation, and the experimental results indicate the validity of the adaptive controller for active vibration isolation [18]. Mehendale et al. utilized linear parameter-varying control techniques to design adaptive active vibration isolation systems for a single degree-of-freedom vibration isolation system [19]. Chen et al. adopted neural network control methods to attenuate external disturbance and isolate vibration in an isolation platform [20]. Xie et al. employed genetic algorithm to isolate vibration of viscoelastic damped structures and verify the applicability of genetic algorithm to vibration isolation of a simple beam structure [21].

The aforementioned works demonstrate that the intelligent control algorithms can improve effect of vibration control. However, the problems of the intelligent control algorithms are twofold. On the one hand, those intelligent control algorithms are sometimes too complex and the computational time of the above algorithms is sometimes very long, which result in limiting their engineering application. On the other hand, control results of the intelligent control algorithms may be different under identical initial parameters. Aimed at such dilemmas, the PID controller which is a direct output feedback method has been widely applied to control vibration. The parameter tuning of the PID controller is the key step in the process of designing the controller. The selection of K_p , K_i and K_d parameters will directly affect the performance of the PID controller. The parameter tuning methods of the PID controller can be divided into experimental method and intelligent tuning method. Zhang et al. chose the appropriate parameters of the PID controller for the isolation platform to reduce the disturbances [22].

The parameter tuning based on the experimental method needs to do many experiments, which is not beneficial for practical engineering application. The intelligent tuning method, an effective PID parameter tuning method, usually used in the PID controller of active isolation systems. Song et al. exploited genetic algorithm to obtain parameters of the PID controller for magnetic suspension system [23]. Fadil et al. employed an iterative learning algorithm to select parameters for the PID controller of flexible beam structure [24]. Rahman et al. utilized ant colony optimization to tune parameters of the PID controller to find optimal required force for wind turbine tower [25]. Although the above intelligent tuning methods make the PID controller have good control performance, the intelligent algorithms are usually complex and time-consuming, which again limits their application. All of the above PID controllers can effectively control vibration based on experimental methods and intelligent tuning methods. However, these aforementioned methods need to conduct many experiments or employ complex algorithms with computation burden and time. For these reasons, the present study investigates an active control method based on equivalent stiffness and damping coefficient, which can be used for practical engineering application.

In this paper, a new active control method with equivalent stiffness and damping coefficient is proposed for the electromagnetic isolation system. In this method, the range of equivalent stiffness coefficient and damping coefficient of the electromagnetic force are calculated based on the required range of dynamic performance indexes. The equivalent stiffness and damping coefficient are similar to the K_p and K_d parameters of a PID controller, which can avoid the parameter tuning problem in the PID controller. According to the established nonlinear relationship between electromagnetic force and coil current and gap in the our own previous paper [26], the equivalent stiffness coefficient and damping coefficient can be satisfied by the controlled current in different gaps for achieving the better vibration isolation performance. Moreover, the control diagram is presented. Finally, simulations and experiments are implemented for verifying the effectiveness of the proposed active control method.

2. Isolation Structure and Electromagnetic Force

The structure of the electromagnetic vibration isolation system is shown in Figure 1, including a spring, two displacement sensors and two electromagnets locate in the spring in order to save space of the isolation system. Some precision instruments might be affected by the motor inside and the disturbance from the external environment. When two electromagnets are passed currents with the identical size but opposite direction, the electromagnetic repulsion force will be generated to attenuate vibration and keep the stability for the isolated object. Due to the fact that two electromagnets connect with spring in parallel, the electromagnetic repulsion force and the elastic force of the spring attenuate vibration together. The changes of displacement produced from the vibration are recorded by two displacement sensors. With the values of displacement, the electromagnetic repulsion force will be transferred to the plate and apply to the vibration source by equivalent stiffness and damping coefficient to control currents.

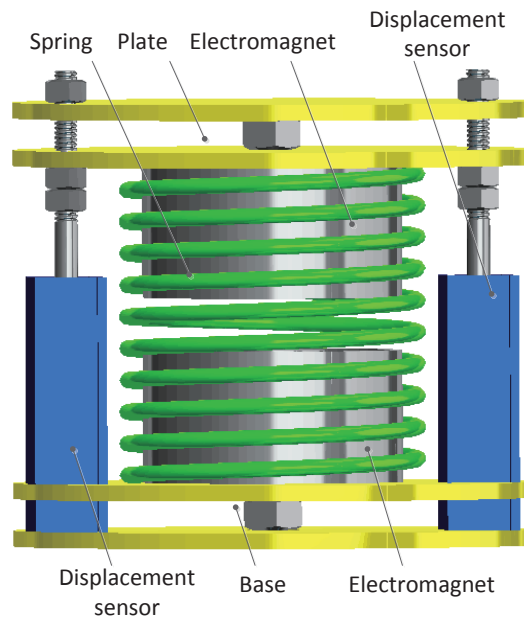


Figure 1. Structure of the electromagnetic isolation system.

Due to the fact that the relationship between electromagnetic force and the gap and coil current with nonlinear characteristics, the electromagnetic vibration isolation system is complex to control. For acquiring the nonlinear relationship between electromagnetic force and the gap and coil current, two electromagnets are simulated by COMSOL Multiphysics when they passed currents with the identical size but opposite direction. There are two cylindrical electromagnets with identical size and parameters in COMSOL Multiphysics. Both two electromagnets are 65 mm in diameter and 30 mm in height. The iron core of the electromagnet is 36 mm in diameter and 30 mm in height. The electromagnet has 2700 rings and the diameter of the coil is 0.53 mm.

Two electromagnets with a 2D axisymmetric model are established by COMSOL Multiphysics. The COMSOL Multiphysics model of two electromagnets is meshed based on free triangular. With the established COMSOL model of two electromagnets, the electromagnetic force can be calculated at any gap and electric current in COMSOL simulation. Based on the COMSOL simulation results, the nonlinear relationship between the electromagnetic force f_e and the gap y and coil current i can be fitted as shown in Equation (1). Equation (1) is obtained by data fitting from COMSOL simulation and verified in experiments which can be referred to [26]. Due to the simulation results in size and varied trend are mainly consistent with the experimental results, the fitting result in Equation (1) is utilized based on the simulation results in this paper:

$$f_e(y, i) = 8259.7863 * y^2 + 2.4055 * i^2 - 61.9546 * y + 3.1128 * i - 311.2811 * y * i - 0.5093 \tag{1}$$

3. Performance Indexes of the Electromagnetic Isolation System

3.1. The Kinetic Equation of an Electromagnetic Isolation System

The model of the vibration isolation system can be simplified in Figure 2, the mass of the electromagnet is m , the damping coefficient of the vibration isolation system when the coil without currents is d_1 and the stiffness of spring is k_1 . The electromagnetic force between two electromagnets is f_e . The plate will

cause the vibration displacement $x(t)$ to emerge after the plate of the system suffers an external force f_d . The downward direction is regarded as the positive direction.

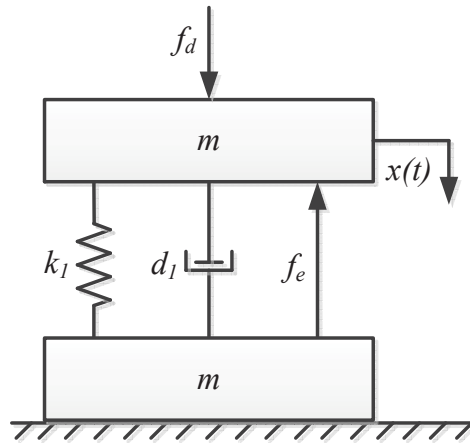


Figure 2. The model of the electromagnetic vibration isolation system.

It is assumed that the condition without currents in two electromagnets is the stable state of the system. The electromagnetic vibration isolation system will become unstable state after the system suffers an external force f_d , which is equal to a step signal in this paper. In order to counteract the external disturbance f_d and get the system back to the stable state, the electromagnetic force f_e is aroused by the controllable currents.

After the system suffers an external force f_d , the kinetic equation of the electromagnetic vibration isolation system can be acquired based on the transfer law of the vibration as follows:

$$M\ddot{x} + d_1\dot{x} + k_1x + f_e(y, i) = f_d \tag{2}$$

where $M = m + m_0$, in which $m = 530$ g is the mass of electromagnet and $m_0 = 200$ g is the mass of an isolated object; $g = 9.8$ N/kg is the gravity of earth; $k_1 = 589$ N/m is the stiffness of spring; $d_1 = 10$ N · s/m is the damping coefficient of the system. The damping coefficient of the vibration isolation system without electric current is determined by experiment, which can be referred to [26].

Due to the fact that the electromagnetic force is determined by the gap y and the current i . The relationship between x and y as follows:

$$y = g(x) = L_0 - 2 * h_0 - x \tag{3}$$

where $L_0 = 0.083$ m is the original length of a spring, $h_0 = 0.03$ m is the height of a electromagnet.

Based on the aforementioned equations, Equation (1) can be changed to keep the unity of the variables as follows:

$$f_e(x, i) = 8259.7863 * x^2 + 2.4055 * i^2 - 317.9956 * x - 4.0467 * i + 311.2811 * x * i + 2.4351 \tag{4}$$

3.2. Relationship between Current and Stiffness and Damping Coefficient

Due to the fact that the two electromagnets with the electromagnetic repulsion force can be simplified as a linear spring or a spring and a damper, the electromagnetic isolation system can be regarded as a

parallel structure consisting of two linear springs or two linear springs and two dampers. In other words, the electromagnetic force could be equal to the following two cases:

- (1) $f_{e1} = k_2x$, in which k_2 is the equivalent stiffness of the two electromagnets. It implies that the two electromagnets with the electromagnetic repulsion force can be simplified as a linear spring. Then, Equation (2) can be rewritten as follows:

$$M\ddot{x} + d_1\dot{x} + (k_1 + k_2)x = f_d \tag{5}$$

The transfer function is achieved by Fourier transforming Equation (5) as follows:

$$G_1(s) = \frac{1}{Ms^2 + d_1s + (k_1 + k_2)} \tag{6}$$

Based on the above transfer function, the damping ratio ζ which is hoped to satisfy $0 < \zeta < 1$ and the undamped natural frequency w_n are respectively obtained as follows:

$$\zeta = \frac{d_1}{2 * M * w_n} \tag{7}$$

$$w_n = \sqrt{\frac{(k_1 + k_2)}{M}} \tag{8}$$

Due to the fact that an object acts on the system is equal to a step input to the electromagnetic vibration isolation system which is a second-order oscillating system. The dynamic performance indexes of the system can be calculated to design the controller as follows:

$$t_r = \frac{\pi - \arccos \zeta}{w_n * \sqrt{1 - \zeta^2}} \tag{9}$$

$$t_p = \frac{\pi}{w_n * \sqrt{1 - \zeta^2}} \tag{10}$$

$$\sigma\% = e^{-\pi * \zeta / \sqrt{1 - \zeta^2}} * 100\% \tag{11}$$

$$t_s = \frac{4}{\zeta * w_n} \tag{12}$$

$$N = \frac{2 * \sqrt{1 - \zeta^2}}{\pi * \zeta} \tag{13}$$

where t_r is the rise time, t_p is the peak time, $\sigma\%$ is the overshoot, t_s is the settling time, and N is the number of oscillations.

Given the desired scopes of performance indexes of the second order system as follows:

$$\left\{ \begin{array}{l} 0 < \zeta < 1 \\ 0 < t_r < 0.1 \\ 0.05 < t_p < 0.2 \\ 0 < \sigma\% < 10\% \\ 0.1 < t_s < 2 \\ 0 < N < 5 \end{array} \right. \tag{14}$$

Based on the above inequalities, the equivalent stiffness k_2 of the two electromagnets can be calculated within a certain range as follows:

$$0 < k_2 < 1151 \tag{15}$$

After the equivalent stiffness k_2 is selected in the above range, the relationship between the equivalent stiffness k_2 and coil current i and the vibration displacement x can be built as follows:

$$f_{e1}(x, i) = 8259.7863 * x^2 + 2.4055 * i^2 - 317.9956 * x - 4.0467 * i + 311.2811 * x * i + 2.4351 = k_2 x \tag{16}$$

Equation (16) indicates that the values of the equivalent stiffness k_2 can be satisfied by controlling the coil currents when the gaps are measured by two displacement sensors. Then, the relationship between current and stiffness is achieved based on the above equation:

- (2) $f_{e2} = k_2 x + d_2 \dot{x}$, in which k_2 is the equivalent stiffness of the two electromagnets, d_2 is the equivalent damping coefficient of the two electromagnets and \dot{x} is the derivative of x . The \dot{x} can be calculated by $[x(k) - x(k - 1)]/T$, in which $x(k)$ is the vibration displacement at time k and T is the control cycle of controller which is equal to 0.01.

It implies that the two electromagnets with the electromagnetic repulsion force can be simplified as a linear spring and a damper. Then, Equation (2) can be rewritten as follows:

$$M\ddot{x} + (d_1 + d_2)\dot{x} + (k_1 + k_2)x = f_d \tag{17}$$

The transfer function is achieved by Fourier transforming Equation (17) as follows:

$$G_2(s) = \frac{1}{Ms^2 + (d_1 + d_2)s + (k_1 + k_2)} \tag{18}$$

The damping ratio ζ which is hoped to satisfy $0 < \zeta < 1$ and the undamped natural frequency w_n are respectively obtained based on Equation (18) as follows:

$$\zeta = \frac{(d_1 + d_2)}{2 * M * w_n} \tag{19}$$

$$w_n = \sqrt{\frac{(k_1 + k_2)}{M}} \tag{20}$$

The dynamic performance indexes of the system can be calculated to design the controller based on Equations (9)–(13). Based on Equation (14), the equivalent stiffness k_2 and the equivalent damping coefficient d_2 of the two electromagnets can be calculated within a certain range as follows:

$$82 < k_2 < 3534 \tag{21}$$

$$17 < d_2 < 109 \tag{22}$$

After the equivalent stiffness k_2 and the equivalent damping coefficient d_2 of the two electromagnets are selected in the above ranges, the relationship between the equivalent stiffness and the equivalent damping coefficient and coil current and the vibration displacement can be built as follows:

$$f_{e2}(y, i) = 8259.7863 * x^2 + 2.4055 * i^2 - 317.9956 * x - 4.0467 * i + 311.2811 * x * i + 2.4351 = k_2 x + d_2 \dot{x} \tag{23}$$

Equation (23) shows that the values of the equivalent stiffness k_2 and the equivalent damping coefficient d_2 can be satisfied by controlling the coil currents when the vibration displacement are measured by two displacement sensors. Then, the relationship between stiffness and damping coefficient and current is obtained based on the above equation.

4. The Control Diagram

The gap between two electromagnets is 0.015 m and the vibration displacement x is 0 m before an external disturbance f_d acts on the electromagnetic vibration isolation system or an isolated object; the system is in a stable state at this time. After the system suffers an external force f_d , the isolated object will cause a vibration displacement x to emerge. In order to counteract the external disturbance and reduce or eliminate the vibration displacement, the electromagnetic force f_e is then aroused through the controllable currents to satisfy the equivalent stiffness or the equivalent stiffness and damping coefficient of the two electromagnets. When the two electromagnets with the electromagnetic forces are simplified as a spring, the equivalent stiffness of the two electromagnets k_2 in Equation (5) is randomly selected as 540 N/m. The equivalent stiffness k_2 and the equivalent damping coefficient of the two electromagnets d_2 are randomly selected as 540 N/m and 30 N · s/m when the two electromagnets with the electromagnetic forces are simplified as a spring and a damper.

With the above analysis and selected parameters, the control diagram is shown in Figure 3, which could be applied for the above active control methods with the equivalent stiffness or the equivalent stiffness and damping coefficient by adjusting parameters. With the calculated equivalent stiffness and damping coefficient based on the required range of dynamic performance indexes, the force between the electromagnets can be achieved according to the measured x and the calculated \dot{x} . The controlled current is then achieved by solving algebraic equation with the vibration displacement in Equation (16) or Equation (23). In the control diagram, the x_r is 0 m, which is the stable state of an electromagnetic isolation system.

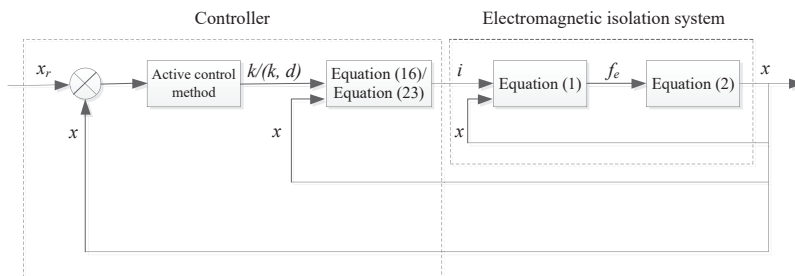


Figure 3. The control diagram with active control methods.

5. Simulation and Experimentation

5.1. Simulation Results

The simulation result with the equivalent stiffness and the simulation result with the equivalent stiffness and damping coefficient are shown in Figure 4; it can be seen that the electromagnetic vibration isolation system is stable at 5.09×10^{-5} m, which is close to 0 m. When the electromagnetic vibration isolation system is controlled by an active method with the equivalent stiffness, the rise time t_r is 0.05 s, the peak time t_p is 0.09 s, the overshoot $\sigma\%$ is 60.7%, the settling time t_s is 1.4 s, and the number of oscillations N is 5. Due to the fact that the range of the overshoot in Equation (14) has no solution, the value of overshoot cannot meet the requirement. However, other performance indexes of the system can satisfy the ranges.

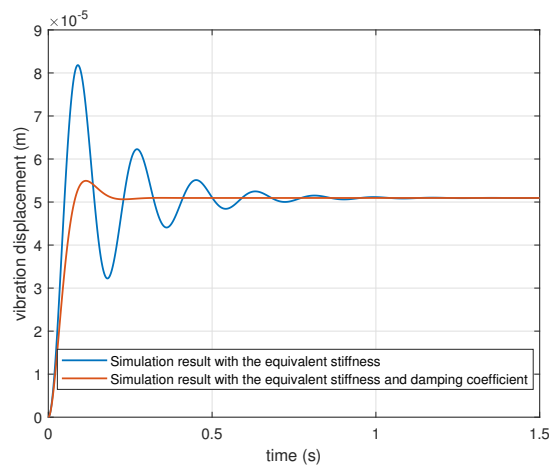


Figure 4. The simulation result with the equivalent stiffness and damping coefficient.

When the electromagnetic vibration isolation system is controlled by active method with the equivalent stiffness and damping coefficient, the vibration displacement x is 5.09×10^{-5} m, the rise time t_r is 0.08 s, the peak time t_p is 0.11 s, the overshoot $\sigma\%$ is 7.9%, the settling time t_s is 0.42 s, and the number of oscillations N is 1. The performance indexes of the electromagnetic vibration isolation system can meet the requirements exactly. It can be seen from the simulation results that the equivalent damping coefficient improves the response time of the electromagnetic isolation system, reduces the overshoot and oscillations, and makes the electromagnetic isolation system have the advantages of fast response and stability, which can meet the real-time requirements of the electromagnetic isolation system in practical application.

5.2. Experimental Results

Experiments are conducted on the electromagnetic vibration isolation system to verify the effectiveness of the proposed active control methods respectively with the equivalent stiffness, with the equivalent stiffness and damping coefficient. Figure 5 shows the physical photo of the electromagnetic vibration isolator system. The digital controller is designed with the proposed active control method and realized on the STM 32 singlechip, which are integrated with data acquisition device on the development board. The C language was used for the programming and the code was compiled and then written into an STM32 chip. All parameters of the isolation system and the mass of the isolated object m_0 are equal to parameters in simulation. Based on the control diagram in Figure 3, the experimental results with the proposed active control methods are shown in Figure 6.

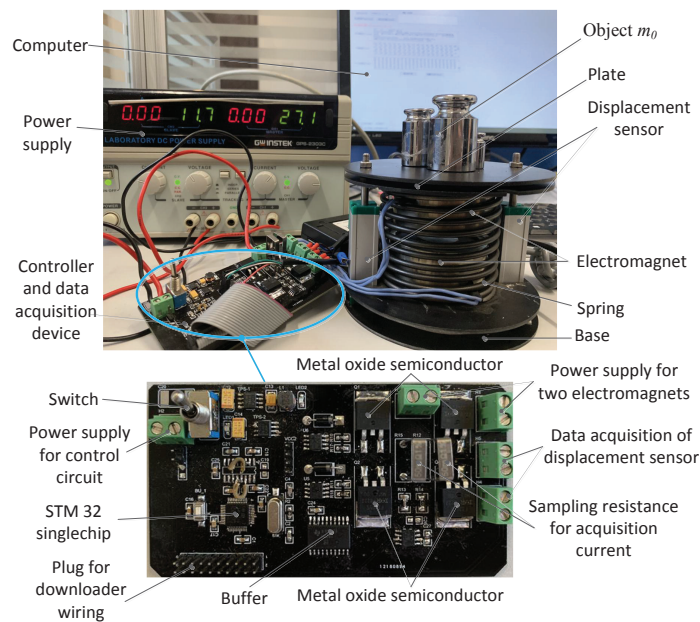


Figure 5. The experimental physical photo.

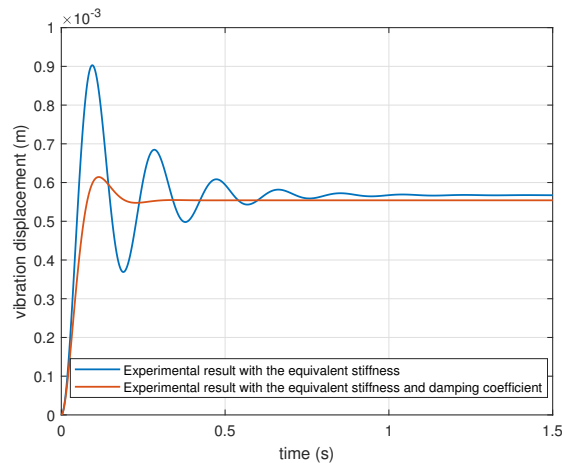


Figure 6. The experimental result with the active control methods.

From Figure 6, it can be seen that the vibration displacement x is stable at 5.67×10^{-4} m based on the active control method with the equivalent stiffness after the system is disturbed by an external force. The rise time t_r is 0.05 s, the peak time t_p is 0.09 s, the overshoot $\sigma\%$ is 59.08%, the settling time t_s is 1.46 s and the number of oscillations N is 5. The vibration displacement x is stable at 5.54×10^{-4} m based on the active control method with the equivalent stiffness and damping coefficient. The rise time t_r is 0.08 s, the peak time t_p is 0.11 s, the overshoot $\sigma\%$ is 9.83%, the settling time t_s is 0.39 s and the number of oscillations N is 1. Although the steady-state errors between the experimental results and the simulation results of the two active control methods are different, it is small enough to be negligible. In addition, the experimental results and the simulation results have the same variation trend. The experimental results demonstrates that the proposed active control methods can effectively control vibration. Compared with the active control approach with the equivalent stiffness, the active control approach with the equivalent stiffness and damping coefficient not only has shorter response time, but also has smaller oscillations and overshoot to ensure the stability of the electromagnetic isolation system and an isolated object.

5.3. Active Control Method with the Piecewise Strategy

Although the active control method with the equivalent stiffness and damping coefficient can effectively control vibration and provide desired dynamic performance indexes, there are overshoot and oscillations in simulation and experimental results. For realizing the variable control parameters of the electromagnetic isolation system and eliminate overshoot and oscillations to keep the stability of the system, an active control method based on the equivalent stiffness and damping coefficient with the piecewise strategy is proposed. From Figure 4, it can be seen that the equivalent damping coefficient shortens the response time of the electromagnetic isolation system, reduces the overshoot and the number of oscillations. However, a smaller equivalent damping coefficient may lead to the overshoot and oscillations of the system, a larger equivalent damping coefficient may increase the settling time, which is not conducive to the real-time requirements in engineering practice. Therefore, the following piecewise strategy is proposed based on the model of electromagnetic isolation system:

- (1) $k_2 = 540 \text{ N/m}, d_2 = 30 \text{ N} \cdot \text{s/m}$, when $x < 4.00 \times 10^{-5} \text{ m}$;
- (2) $k_2 = 540 \text{ N/m}, d_2 = 70 \text{ N} \cdot \text{s/m}$, when $x \geq 4.00 \times 10^{-5} \text{ m}$.

The plate will produce the vibration displacement x after the plate of the electromagnetic vibration isolation system suffer an external force, the controlled current is then aroused by solving algebraic Equation (23) with the equivalent stiffness and damping coefficient based on the piecewise strategy to offset the external force and keep the stability of the system. The control diagram with the active control method based on the piecewise equivalent stiffness and damping coefficient is shown in Figure 7. According to the vibration displacements are measured by the displacement sensor, various equivalent stiffness and damping coefficients could be conducted. With Equations (1) and (2), the controlled currents are then achieved by solving algebraic equation with the vibration displacement in Equation (23).

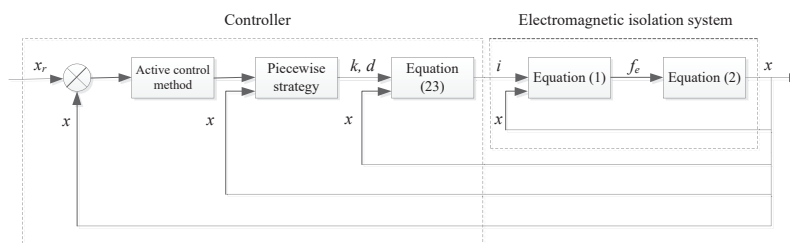


Figure 7. The control diagram with the piecewise strategy.

In order to verify the advantages of the active control method based on the piecewise equivalent stiffness and damping coefficient, the the method based on the fixed equivalent stiffness $k_2 = 540 \text{ N/m}$ and fixed equivalent damping coefficient $d_2 = 70 \text{ N} \cdot \text{s/m}$ is utilized for comparison purpose. Figure 8 shows the comparison results, when the electromagnetic isolation system is controlled by active method with the piecewise equivalent stiffness and damping coefficient, the vibration displacement x is stable at $5.09 \times 10^{-5} \text{ m}$ which is close to 0 m , the rise time t_r , the peak time t_p and the settling time t_s are both equal to 0.32 s , the overshoot $\sigma\%$ and the number of oscillations N are both equal to 0 . When the electromagnetic isolation system is controlled by active method with the fixed equivalent stiffness $k_2 = 540 \text{ N/m}$ and fixed equivalent damping coefficient $d_2 = 70 \text{ N} \cdot \text{s/m}$, the overshoot $\sigma\%$ and the number of oscillations N are both equal to 0 , and the vibration displacement x is stable at $5.09 \times 10^{-5} \text{ m}$; however, the rise time t_r , the peak time t_p , and the settling time t_s are both equal to 0.58 s . The simulation results show that the equivalent damping coefficient can reduce the overshoot and the number of oscillations, and ensure the stability of the system; however, an excessive equivalent damping coefficient may increase the settling

time. The active control approach with the piecewise equivalent stiffness and damping coefficient can not only keep the system have a shorter settling time, but also keep the stability of the electromagnetic isolation system and an isolated object, which can meet the requirements of the electromagnetic vibration isolation system in practical application.

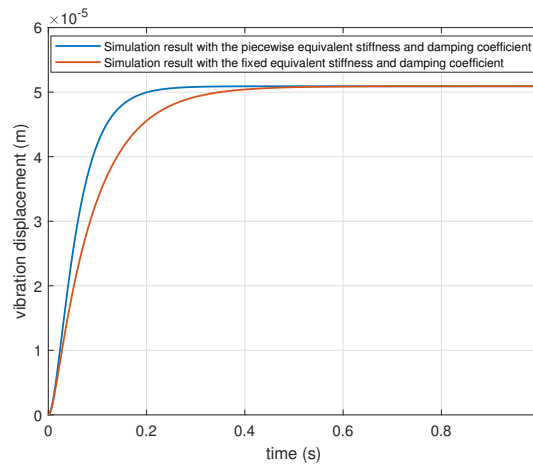


Figure 8. Simulation results of two active control methods.

Based on the experimental result in Figure 6, the active control method with the equivalent stiffness and damping coefficient can effectively control vibration and provide desired dynamic performance indexes. However, there are overshoot and oscillations in experimental results. In order to reduce overshoot and oscillations to keep the stability of the electromagnetic isolation system and an isolated object, the piecewise strategy is proposed as follows:

- (1) $k_2 = 540 \text{ N/m}, d_2 = 30 \text{ N} \cdot \text{s/m}$, when $x < 4.00 \times 10^{-4} \text{ m}$;
- (2) $k_2 = 540 \text{ N/m}, d_2 = 70 \text{ N} \cdot \text{s/m}$, when $x \geq 4.00 \times 10^{-4} \text{ m}$.

The method based on the fixed equivalent stiffness $k_2 = 540 \text{ N/m}$ and fixed equivalent damping coefficient $d_2 = 70 \text{ N} \cdot \text{s/m}$ is utilized for comparison purpose in experiments. Figure 9 shows the comparison results from experiments, when the system is controlled by active method with the piecewise equivalent stiffness and damping coefficient, the vibration displacement x is stable at $5.54 \times 10^{-4} \text{ m}$, the rise time t_r , the peak time t_p and the settling time t_s are both equal to 0.44 s, the overshoot $\sigma\%$ and the number of oscillations N are both equal to 0. When the system is controlled by the active approach with the fixed equivalent stiffness and fixed equivalent damping coefficient, the vibration displacement x is stable at $5.54 \times 10^{-4} \text{ m}$, the overshoot $\sigma\%$ and the number of oscillations N are both equal to 0, however the rise time t_r , the peak time t_p and the settling time t_s are both equal to 0.69 s. The experimental results verify the simulation results, which demonstrate that the active control approach with the piecewise equivalent stiffness and damping coefficient can not only improve the response speed of the system, but also keep the stability of the system and an isolated object.

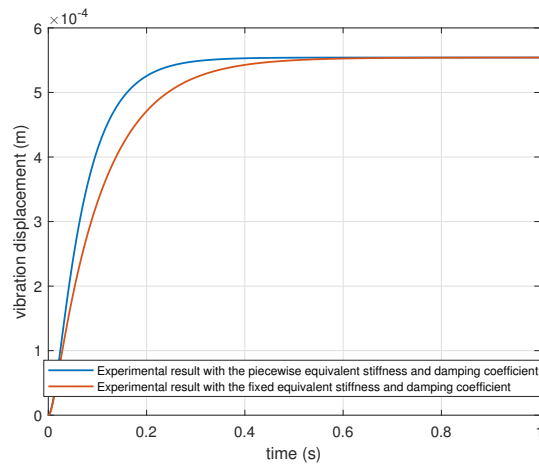


Figure 9. Experimental results of two active control methods.

6. Conclusions

The vibration control method, a significant concern in the electromagnetic isolation system, can bring controllable stiffness and damping coefficient, and fast response. For improving the performance of an electromagnetic isolation system with reasonable parameters and avoid the parameter tuning problem of a PID controller, an active control method is put forward based on equivalent stiffness and damping coefficient. The equivalent stiffness and damping coefficient are similar to the K_p and K_d parameters of a PID controller. The conclusions are obtained in this paper are as follows:

- (1) Due to the two electromagnets with the electromagnetic force could be simplified as a spring or a spring and a damper, the equivalent stiffness coefficient and damping coefficient of the electromagnetic isolation system are calculated by the required range of dynamic performance indexes, which can avoid the parameter tuning problem of a PID controller. According to the established nonlinear relationship, the equivalent stiffness and the equivalent damping coefficient can be satisfied by controlling the coil currents. Based on the model of the system and the proposed active control method, the control diagrams are established for simulations and experiments.
- (2) The simulation and experimental results verify that the active control approach with the equivalent stiffness and damping coefficient can obtain the desired dynamic performance indexes and control vibration amplitudes for keeping stability of the isolation system.
- (3) In order to realize the variable control parameters of the electromagnetic vibration isolation system and eliminate overshoot and oscillations, an active control method based on the equivalent stiffness and damping coefficient with the piecewise strategy is proposed. The simulation and experimental results show that the control method based on the piecewise equivalent stiffness and damping coefficient can not only reduce the setting time of the system, but also ensure the stability of the system. The conclusion is useful for vibration control in the active electromagnetic isolation system in practical engineering.

Author Contributions: L.Z. conceived method; L.Z. and X.Z. designed and performed the experiments; L.Z. analyzed the simulation and experimental data; L.Z. and X.Z. wrote the paper. All authors have read and agreed to the published version of the manuscript.

Funding: This work was supported by Basic Research Project of the Knowledge Innovation Program in Shenzhen under Grant JCYJ20170818144449801.

Conflicts of Interest: The authors declare no conflict of interest.

References

1. Daley, S.; Johnson, F.A.; Pearson, J.B.; Dixon, R. Active vibration control for marine applications. *Control Eng. Pract.* **2004**, *12*, 465–474.
2. Robertson, W.; Kinder, M.R.F.; Cazzolato, B.; Zander, A. Theoretical design parameters for a quasi-zero stiffness magnetic spring for vibration isolation. *J. Sound Vib.* **2009**, *326*, 88–103.
3. Wang, R.C.; Ding, R.K.; Chen, L. Application of hybrid electromagnetic suspension in vibration energy regeneration and active control. *J. Vib. Control* **2018**, *24*, 223–233.
4. Zheng, L.; Huang, B.; Zhang, Q.; Lu, X.L. Experimental and analytical study on vibration control effects of eddy-current tuned mass dampers under seismic excitations. *J. Sound Vib.* **2018**, *24*, 153–165.
5. Hoque, M.E.; Takasaki, M.; Ishino, Y.; Suzuki, H.H.; Mizuno, T. An active micro vibration isolation with zero-power controlled magnetic suspension technology. *JSME Int. J. Ser. Mech. Syst. Mach. Elem. Manuf.* **2006**, *49*, 719–726.
6. Chen, J.D.; Lu, G.T.; Li, Y.R.; Wang, T.; Wang, W.X.; Song, G.B. Experimental study on robustness of an eddy current-tuned mass damper. *Appl. Sci.* **2017**, *7*, 895.
7. Yip, W.S.; To, S. Tool life enhancement in dry diamond turning of titanium alloys using an eddy current damping and a magnetic field for sustainable manufacturing. *J. Clean. Prod.* **2017**, *168*, 929–939.
8. Amjadian, M.; Agrawal, A.K. A passive electromagnetic eddy current friction damper (PEMECFD): Theoretical and analytical modeling. *Struct. Control Health Monit.* **2017**, *24*, 1978.
9. Setareh, M.; Hanson, R.D. Tuned mass dampers to control floor vibration from humans. *J. Struct. Eng.* **1992**, *118*, 741–762.
10. Antoniadis, I.A.; Kanarachos, S.A.; Gryllias, K.; Sapountzakis, I.E. KDamping: A stiffness based vibration absorption concept. *J. Vib. Control* **2018**, *24*, 588–606.
11. Ahn, H.J.; Hwang, K.; Nguyen, D.C. Eddy current damper for passive reaction force compensation of a linear motor motion stage. *Proc. Inst. Mech. Eng. Part J. Syst. Control Eng.* **2017**, *231*, 360–366.
12. Bae, J.S.; Hwang, J.H.; Roh, J.H.; Kim, J.H.; Yi, M.S.; Lim, J.H. Vibration suppression of a cantilever beam using magnetically tuned-mass-damper. *J. Sound Vib.* **2012**, *331*, 5669–5684.
13. Kim, H.T.; Lee, K.W.; Kim, C.H.; Lee, G.S. An electro-magneto-pneumatic spring for vibration control in semiconductor manufacturing. In Proceedings of the IEEE International Conference on Mechatronics, Malaga, Spain, 14–17 April 2009; pp. 1–6.
14. Zhou, N.; Liu, K. A tunable high-static-low-dynamic stiffness vibration isolation. *J. Sound Vib.* **2010**, *329*, 1254–1273.
15. Ahn, K.G.; Pakh, H.J.; Jung, M.Y.; Cho, D.W. A hybrid-type active vibration isolation system using neural networks. *J. Sound Vib.* **1996**, *4*, 793–805.
16. Sun, T.; Huang, Z.; Chen, D. Signal frequency-based semi-active fuzzy control for two-stage vibration isolation system. *J. Sound Vib.* **2005**, *280*, 965–981.
17. Bai, M.R.; Liu, W. Control design of active vibration isolation using μ -synthesis. *J. Sound Vib.* **2002**, *257*, 157–175.
18. Shaw, J. Active vibration isolation by adaptive control. *J. Vib. Control* **2011**, *7*, 19–31.
19. Mehendale, C.S.; Fialho, I.J.; Grigoriadis, K.M. A linear parameter-varying framework for adaptive active microgravity isolation. *J. Vib. Control* **2009**, *15*, 773–800.
20. Chen, K.T.; Chou, C.H.; Chang, S.H.; Liu, Y.H. Intelligent active vibration control in an isolation platform. *Appl. Acoust.* **2007**, *69*, 1063–1084.
21. Xie, Z.; Shepard, W.S.; Woodbury, K.A. Design optimization for vibration reduction of viscoelastic damped structures using genetic algorithms. *Shock Vib.* **2009**, *16*, 455–466.
22. Zhang, Y.; Xu, S.J. Vibration isolation platform for control moment gyroscopes on satellites. *J. Aerosp. Eng.* **2012**, *25*, 641–652. [[CrossRef](#)]
23. Song, F.Z.; Liu, H.; Song, B.; Feng, H.M. Dynamic optimization of PID control parameters of complex magnetic suspension electromechanical coupling system. In Proceedings of the 2010 8th World Congress on Intelligent Control and Automation, Jinan, China, 7–9 July 2010; pp. 3435–3440.

24. Fadil, M.A.; Jalil, N.A.; Darus, I.Z.M. Intelligent PID controller using iterative learning algorithm for active vibration controller of flexible beam. In Proceedings of the 2013 IEEE Symposium on Computers and Informatics, Langkawi, Malaysia, 7–9 April 2013.
25. Rahman, M.; Ong, Z.C.; Chong, W.T.; Julai, S.; Ng, X.W. Wind turbine tower modeling and vibration control under different types of loads using ant colony optimized PID controller. *Arab. J. Sci. Eng.* **2019**, *44*, 707–720. [[CrossRef](#)]
26. Zhang, L.; Zhuan, X.T. An experimental study of an electromagnetic isolator system with active control. *Int. J. Appl. Electromagn. Mech.* **2019**, *61*, 329–340. [[CrossRef](#)]

Publisher’s Note: MDPI stays neutral with regard to jurisdictional claims in published maps and institutional affiliations.



© 2020 by the authors. Licensee MDPI, Basel, Switzerland. This article is an open access article distributed under the terms and conditions of the Creative Commons Attribution (CC BY) license (<http://creativecommons.org/licenses/by/4.0/>).